Biogas upgrading with novel cellulose nano-crystals and polyvinyl amine nanocomposite membranes

Uzair Saeed[a], Zaib Jahan[a,*], Muhammad Bilal Khan Niazi[a], Erum Pervaiz[a], Farooq Sher[b]

[a]*Department of Chemical Engineering, School of Chemical and Materials Engineering, National University of Sciences and Technology, Islamabad, Pakistan*

[b]*School of Mechanical, Aerospace and Automotive Engineering, Faculty of Engineering, Environmental and Computing, Coventry University, Coventry CV1 5FB, United Kingdom*

*Corresponding author:

Email: zaibjahan@scme.nut.edu.pk (Z. Jahan)

Tel.: +92 51 90855080

Postal address: School of Chemical and Materials Engineering, National University of Sciences and Technology

Islamabad

Pakistan

Abstract

A novel crystalline nano cellulose (CNC) and polyvinyl amine (PVAm) based nanocomposite membranes were synthesized and evaluated for biogas upgrading. Different concentrations of CNC was incorporated in 3wt % PVAm solution on commercial polysulfone (PSf) sheet using dip coating method. The effect of feed pressure (5, 10 and 15 bar) was investigated for the CO_2/CH_4 separation. The incorporation of CNC increased the crystallinity of membranes. The thickness of selective layer enhanced to 2.16 μm from 1.5 μm with increasing concentration of CNC. However, degree of swelling reduced from 75.88% to 68.93 with CNC concentration at 1.5 wt.%. The best results were shown by PVAm membrane with 1 wt. % CNC concentration i.e. CO_2 permeance of 0.0216 $m^3(STP)/m^2.bar.hr$ and selectivity (CO_2/CH_4) of 41.The permeance decreased approximately 1.8 folds for PVAm/1CNC membrane with the increase in pressure from 5 to 15 bar. However, selectivity dropped from 41 to 39 for formulated membranes.

Keywords: Polyvinyl amine; Cellulose nano-crystals; Biogas upgrading; Nanocomposite membranes; Fixed site carrier membranes.

1 Introduction

Reduction in Greenhouse gas (GHG) emission is driving the global concerns due to its profound impacts on our climate. Carbon dioxide (CO_2) a primary greenhouse gas, is mainly produced by burning of fuels and is estimated that the amount of CO_2 will increased to 37 Gt by 2035 [1]. Currently, 80% of world's energy demands are fulfilled by fossil fuels. If we follow the same trend, fossil fuels reservoirs will be consumed in approximately the next 100 years [2].

Furthermore, in order to limit global warming, it is required that energy use would have to be totally decarbonizes and renewable must provide 65% of global energy demands by 2050 [3]. Therefore, it is necessary to find the sustainable and renewable energy resources with low carbon emission. Currently, 18.6% of total world's energy demands are being fulfilled by renewable energy sources. However, bioenergy accounts for approximately 14% [4]. Hence, bioenergy would be expected to the most potential and sustainable source of renewable energy for future global primary energy mix in 2050 [5].

Biogas is a form of bioenergy and product of Anaerobic Digestion (decomposition in an oxygen deficient environment) of organic waste. It is mainly comprising of CH_4 (50-70) % and CO_2 (30-50) %. The relative concentration of these two gases largely depends on nature of raw material and pH of bioreactor [6]. Biogas is being used for heating, production of steam and generation of electricity. However, after improving energy contents it can also be used as fuel for vehicles and grid stations. Presences of CO_2, mainly reduces the calorific value of biogas and limit its utilization. Upgraded biogas is also called as bio methane (>95 % CH4 contents) and can meet the technical requirements to replace the natural gas. Furthermore, the bio methane fuel has potential to reduce the non-methane volatile organic compounds emission by 50% and NO_X emissions by 25%. Furthermore, a significant reduction in particulate emission [7].

Biogas is upgraded by various techniques such as; water or amine scrubbing, pressure swing adsorption, membrane technology, and absorption [2]. The membrane separation is a proven green technology with cost effective CO_2 capture solution, and reduced footprints. Membrane technology has also been proven beneficial for low gas volumes and high CO_2 contents [8].

Therefore, membrane technology is highly recommended for the biogas upgrading by CO_2 removal [9].Various strategies have been employed in past to manufacture polymeric membrane with high efficiency, cost effectiveness and ease of fabrication. However, due to transport mechanism mainly based molecular sieving and kinetic diameter, the inherent trade-off between selectivity and permeability of polymeric membranes is a challenge. Therefore, to overcome this limitation, Facilitated Transport Membranes (FTM) were first introduced as Supported Liquid Membranes (SLM). The moveable carriers react with dissolved CO_2. This complex is then transported across the membrane by solution diffusion mechanism. However, leakage of carrier in permeate and loss of solution by evaporation reduced the membrane performance with time. To overcome this problem, a new class of membranes has been evolved known as Fixed Site Carrier (FSC) membranes [10, 11].

In FSC, the carrier is covalently bounded to the main polymer matrix. However, it reduced the free mobility of carrier but enhanced the overall stability and performance of membranes. Recently, research has been focused to make membrane material more hydrophilic to take the advantage of liquid membranes in highly swollen conditions [12-15]. The FTM that works under highly swollen conditions facilitate the CO_2 transport as bicarbonate ion (HCO_3^-) through the membrane [16]. Utilization of such membranes have been reported in the literature and is revealed from the results that the degree of swelling is directly related to membrane performance [15, 17, 18]. Furthermore, number of nano filler and carrier molecules has been incorporated to enhanced swelling as well as affinity of composite membranes for CO_2 [13, 19].

Among different polymers used for acid gas separation, the polyvinyl amine is the most promising one. Due to the presence of abundant amine group and high degree of hydrophilicity, it gives high permeability and selectivity for CO_2. Furthermore, PVAm is easily soluble in the water at room temperature [10, 20]. PVAm has been extensively investigated for CO_2 separation applications alone or with different combinations of fillers in mixed matrix membranes [10, 12, 21, 22]. The structure of PVAm consists of amine group in its chain ($-NH_2$) which has a natural affinity for CO_2. It acts as fixed site carriers and facilitate transport of CO_2 across the membrane. Recently, Zhao et al. has used PVAm in mixed matrix composite membranes with PANI/PS and results showed that the presence of PANI nanoparticles in PVAm matrix enhanced separation performance of composite membranes [23]. Further, Ming Wang and Zhi Wang et al. incorporated inorganic fillers such as MWCNT, SiO_2 and ZSM-5 and study their interfacial properties. The study suggested that addition of nanofillers to PVAm matrix is an effective way to improve interfacial properties. However, better results could be obtained if inorganic filler and polymer has same functional groups [22]. But, stability issues of PVAm particularly at high pressure can be overcome by using high molecular weight PVAm or by introducing finely dispersed second phase in polymer matrix with high mechanical strength.

The Crystalline Nano cellulose (CNC) has been used in this research due to its high affinity with water and reinforcing nature [13, 24-27]. Cellulose fibers have hierarchical microstructures and on acid hydrolysis give nanostructure of highly crystalline regions (CNC) and amorphous regions (CNF) [13, 28-30]. D- glucopyranose ($C_6H_{11}O_5$) is a major component associated by β (1,4) links which is the repeating unit of cellulose [31]. The degree of polymerization of cellulose is difficult to determine but is reported to be near 10,000 if the molecular weight is around 3.2×10^6 g/mol.

CNCs have become the center of attention for researchers due to its unique properties that include outstanding mechanical attributes, reinforcing capabilities, low density, biodegradability and excellent surface area per unit mass[13, 18, 24, 28]. Moreover, cellulose is being abundantly used in bio and nanocomposites. Due to biodegradable nature, cellulose has replaced multiple synthetic fibers which also contribute in polluting environment. Cellulose is also being used as nonstructural biocomposite in doors, windows, ceiling tiles etc. [32]. Recently, CNCs have been reported as an additive with PVA and showed enhanced results of CO_2 separation up to 15 bars. Furthermore, NFC has also been reported for enhanced performance of composite membranes. CNCs disperse along the polymeric matrix and help in moisture uptake and promotes swelling. This moisture content helps to increase the rate of facilitated transport of CO_2 across the membrane [18]. Furthermore, PVA has also been chemically cross-linked with CNCs resulting in excellent thermal stability and reinforcement capability. Cross-linked PVA/CNCs have also been utilized in biocompatible electronic skin sensor system [33, 34].

Thermodynamic properties of polymers play a vital role in the separation performance of membranes. Flory-Huggins theory describes the thermodynamics of polymer solutions and blends. It is a lattice model that explains the non-ideality of polymer mixtures. Comprehensive thermodynamic studies of polymeric blends have been carried out by Rana et al., for example, polyvinyl esters and polyacrylates, polystyrene-co-acrylonitrile and polyphenyl acrylate etc. Hydrogenated polymers were used as analogues of respective polymers and interaction energy densities were calculated [35-37]. However, in this work, polysulfone (PSf) and PVAm does not form blend and are chemically inert. Therefore, thermodynamics of these polymers have not been covered in this work.

This research work is carried out to improve the mechanical properties and water affinity of PVAm membranes to enhance CO_2 separation at moderately high pressures. CNC has been incorporated in PVAm matrix in order to get beneficial results. There has been no chemical crosslinking between PVAm and CNC. The membranes were investigated for the optimized concentration of CNC in 3% PVAm solution. Effect of addition of different concentrations of CNC on degree of swelling was investigated. The SEM analysis of membranes was conducted to find the effect of incorporation of CNC on morphology and thickness of selective layer. The effect on degree of crystallinity of PVAm/CNC nanocomposite membranes was investigated using XRD. The membrane rig used for CO_2 permeation testing was specially designed and has ability to work under humid conditions at moderately high pressure. Membranes were investigated under highly swollen conditions at 5, 10 and 15 bars. The results will be interpreted in terms of permeance of CO_2 and CH_4 and selectivity of CO_2/CH_4.

2 Experimental

2.1 Materials

Ultrafiltration flat sheet membrane of Polysulfone (PSf) (Molecular weight cut-off 50,000) of the commercial grade was purchased from Alfa Laval. CNCs were acquired from Cellulose Lab, Canada. The average width and length of CNC was 12nm and 170nm, respectively. Polyvinyl amine (MW 17,000-20,000) was purchased from Sigma Scientific. The solvent used for casting of membranes was deionized water.

2.2 Preparation of composite membrane

PVAm was added to deionized water and stirred for 3 hours to get 3 wt. % solution of polyvinyl amine. The mixture was left for rolling on mechanical roller overnight to obtain a clear solution. This procedure was carried out at room temperature. Afterwards, CNCs were added to the clear solution [38]. Different concentrations of CNCs with respect to weight percent of polymer i.e. 0.5%, 1% and 1.5%, were added to get casting solutions as shown in Table 1. The solutions were mechanically stirred overnight and sonicated afterwards for 30 min. The air bubbles should be removed from resultant suspension to cast defect free membranes. Therefore, solution was left at room temperature for 2 hours. .Using a dip-coating technique, a selective and dense membrane was casted on PSf sheet as shown in Figure 1. The membranes were placed in fume hood overnight at room temperature for drying. [10].

Table.1: Composition of casted membranes with their codes.

Membrane code	PVAm wt. %	Wt./Wt. CNC
Pure PVAm	3 g	-
PVAm/0.5CNC	3 g	0.5 %
PVAm/1CNC	3 g	1 %
PVAm/1.5CNC	3 g	1.5 %

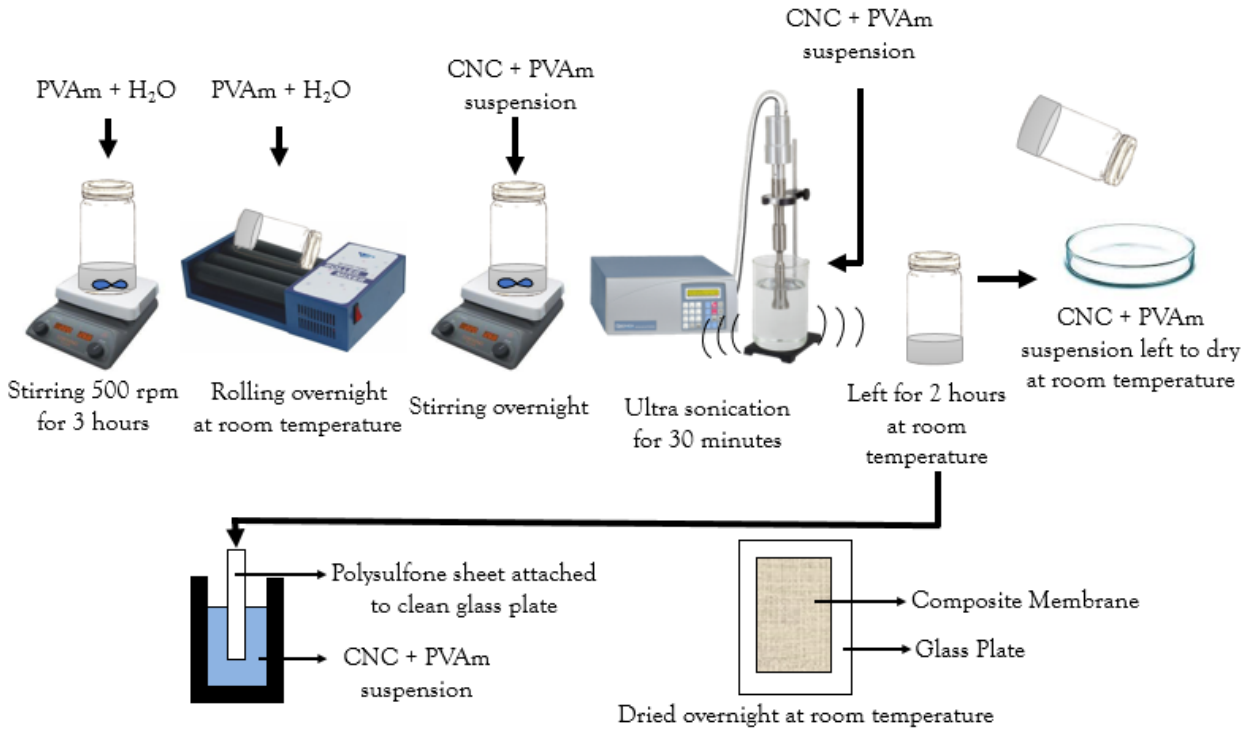

Figure1. Cellulose nano-crystals and polyvinyl amine nanocomposite membranes.

2.3 Scanning electron microscopy

The morphology of nanocomposite membranes was investigated by using Scanning Electron Microscopy (S-4700 Hitachi, Japan). The gold sputtering was carried out on membranes by ion sputtering machine model JFC-1500 JEOL Limited. In order to find the thickness of selective layer of membrane over polysulfone sheet, cross sectional view of membranes were also examined. Liquid nitrogen was used to break membrane for the cross-sectional images.

2.4 X-ray diffraction

The crystallinity of nanocomposite membranes was determined by using STOE X-ray Diffractometer. The scan angle was set to 20-60° at a step size of 0.4° and a step time of 0.5 sec/step. The radiation energy used for x-ray diffraction was Cu K α-1 frequency of 1.5406 Å. The

method mentioned in literature was used to determine the crystallinity index of casted membranes [39]. The area under the curve of the XRD spectrum between 20-60° was considered as total area.

2.5 Percentage moisture uptake

The degree of swelling of PVAm/CNC membranes was investigated at room temperature by subjecting them to a humid environment. The membranes were placed in a closed chamber with relative humidity (RH) of 0%. The degree of swelling of membranes was measured by subjecting them to environment with87% relative humidity. The membranes were placed in such a way that there was no direct contact of membranes with the saturated salt solution. The degree of swelling was calculated after every 24 hours on basis of the increase in weight of membranes. The readings were taken for 10 days. Day 1 measurement was taken after 24 hours in which membranes were subjected from 0% RH to 87% RH. Equation (1) was used to calculate the degree of swelling [14].

$$DoS\ (\%) = \frac{S-D}{D} X\ 100 \quad (1)$$

Where, D is the mass of dry membrane and S is the mass of swelled membranes.

2.6 Permeation test

Permeation testing was conducted to examine the performance of membrane for CO_2 capture. A membrane rig as shown in Figure 2 was used to conduct permeation testing. The rig has ability to test the membranes at moderately high pressures; up to 20 bars at both humid and dry conditions. Figure 2 shows the flow diagram of membrane rig.

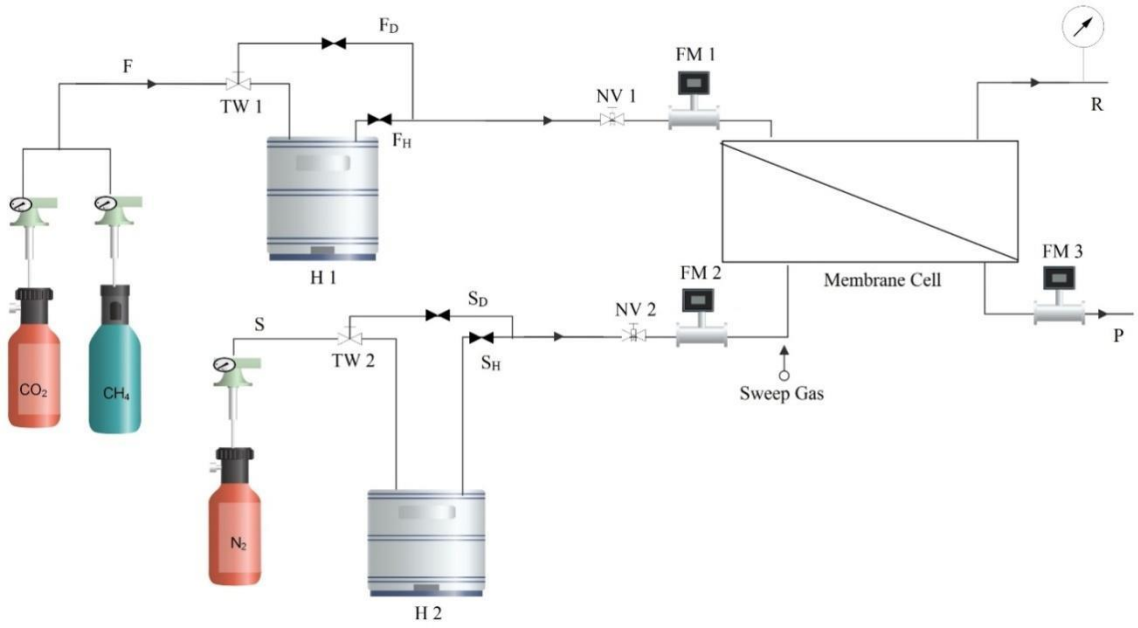

196

197 **Figure 2.** Flow diagram of gas permeation rig, F = Feed Line, S = Sweep Line, TW = Two Way
198 Valve, F_D = Dry Feed, F_H = Humidified Feed, S_D = Dry Sweep, S_H = Humidified Sweep, H =
199 Humidifier, NV = Needle Valve, FM = Flow Meter, P = Permeate, R = Retentate.
200

201 CO_2 or CH_4 are filled in cylinders which are allowed to flow in feed line, F, controlled by the
202 pressure regulators attached with cylinders. After leaving the cylinder, gas moves towards a two-
203 way valve which provides an option for the gas to be used in dry conditions, F_D, or in humidified
204 conditions, F_H. For dry gas, humidifier, H1, is bypassed. Needle valve NV1 is present, which
205 allows precise control of gas flow. Flow meter, FM1, indicates the flow rate of feed gas before
206 entering to membrane cell. The gas that pass through the membrane, exits the cell from bottom as
207 permeate, P. While that do not pass the membrane, exits from top as retentate, R. Flow rate of
208 permeate is measured manually by bubble flow meter indicated here as FM3.
209

N_2 is used as the sweep gas. The pressure is controlled and read using pressure regulator and gauge, respectively. Same phenomenon as above takes place in sweep line. Two-way valve, TW2, allows either sweep be humidified, S_H, or dry, S_D. Volume of humidifier is the same as for above. Needle valve, NV2, and flow meter, FM2, controls and measures the flow rate of sweep gas, respectively. However, sweep enters the membrane cell from bottom and exits the permeate line P. The pressure and flow of sweep gas are kept very low. Different membrane compositions were tested for their CO_2 and CH_4 permeability and selectivity. Sweep gas was humidified and then supplied to membranes so that maximum moisture uptake was achieved as indicated by the degree of swelling of membranes. The single gas testing for CO_2 and CH_4 were carried out by supplying the humid gases to the membranes. Effect of pressure was investigated by supplying feed gases at 5, 10 and 15 bar. While, keeping flow rate and temperature constant. The permeability of the gases was measured manually by using a bubble flow meter.

3 Results and discussion

3.1 Characterization

3.1.1 Morphology and thickness of composite membranes

The scanning electron microscopy (SEM) analysis was performed to investigate the morphology and thickness of selective layer. SEM results revealed the smooth and defect free surface of PVAm/1CNC membrane as shown in Figure 3(a). Furthermore, no agglomeration of nano particles was observed on the membrane surface. This indicates the even dispersion of nano particles within the polymeric matrix. Moreover, no cracks are visible on the membrane surface. Hence, the surface morphology does not show any adverse effect with addition of CNC. The cross sectional view of PVAm/1CNC composite membrane are represented in Figure 3(b). Web like structure refers to the

micro-porous PSf support with selective PVAm/CNC membrane on the top. Membrane thickness was determined by taking measurements at different parts of the composite membrane. The average thickness observed for PVAm/1CNC membrane was approximately 1.5±0.12µm. Furthermore, the selective layer thickness enhanced with increase in the concentration of CNC in the polymeric membrane as shown in figure 3(c). This can be ascribed to the increase in viscosity of the casting solution with increasing the CNC concentration. The addition of 1.5wt % CNC increases the average thickness of membrane three times of the thickness of pure PVAm membrane. However, 1wt% CNC membrane shows optimized results with thickness of 1500 nm. Hence, an increment in membrane thickness is observed for a successive increase in CNC concentration [40].

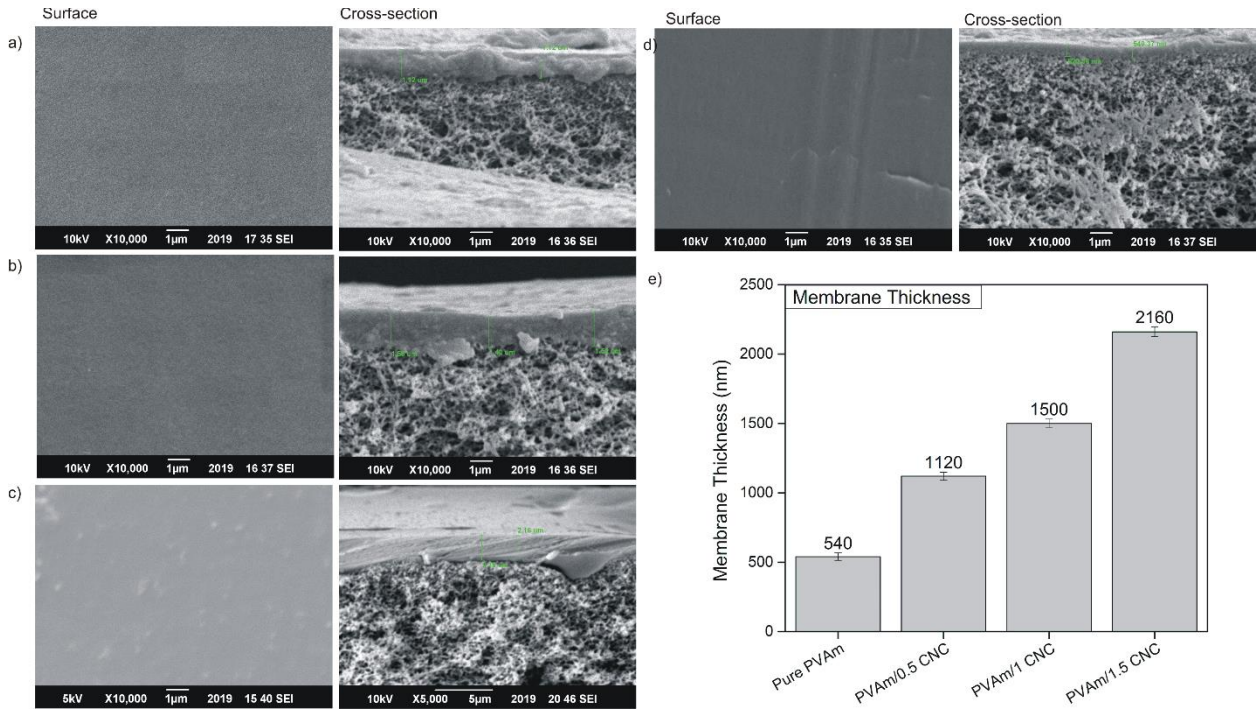

Figure 3. SEM images of PVAm/CNC membranes with addition of 1 wt% CNC, (a) surface and cross-section morphology of PVAm/0.5CNC, (b) surface and cross-section morphology of PVAm/1CNC, (c) surface and cross-section morphology of PVAm/1.5CNC, (d) surface and cross-section morphology of pure PVAm membrane, and (e) thickness of nanocomposite membranes.

3.1.2 Swelling behavior

Degree of swelling of composite membranes was investigated by subjecting them to a RH of 87%. Figure4 (a) shows the maximum moisture uptake over a period of 10 days. The maximum swelling was observed until day 5. However, the membrane with 1% CNC concentration absorbed the moisture until day 6. Furthermore, a gradual increase in the degree of swelling was observed for pure PVAm membrane between day 6 and 7. The highest degree of swelling was observed for membrane with 1% CNC concentration i.e. 75.88±1.1%. However, the membrane with 1.5% CNC contents showed a swelling percentage of 68.93±0.9%. The strong reinforcement capability of CNC molecules result in reduced degree of swelling when CNC concentration is increased. This effect resists the mechanical restraining and rejects the further uptake of water molecules resulting in a reduced degree of swelling of PVAm/CNC composite membranes [18]. Increasing CNC concentration imparts strong hydrogen bonding which affixes the polymeric chains thus reducing the moisture uptake capability of membranes [41]. Moreover, reduction in swelling degree can also be correlated with the rise in the crystallinity index of membranes with the increasing CNC concentrations as shown in figure 4(b).

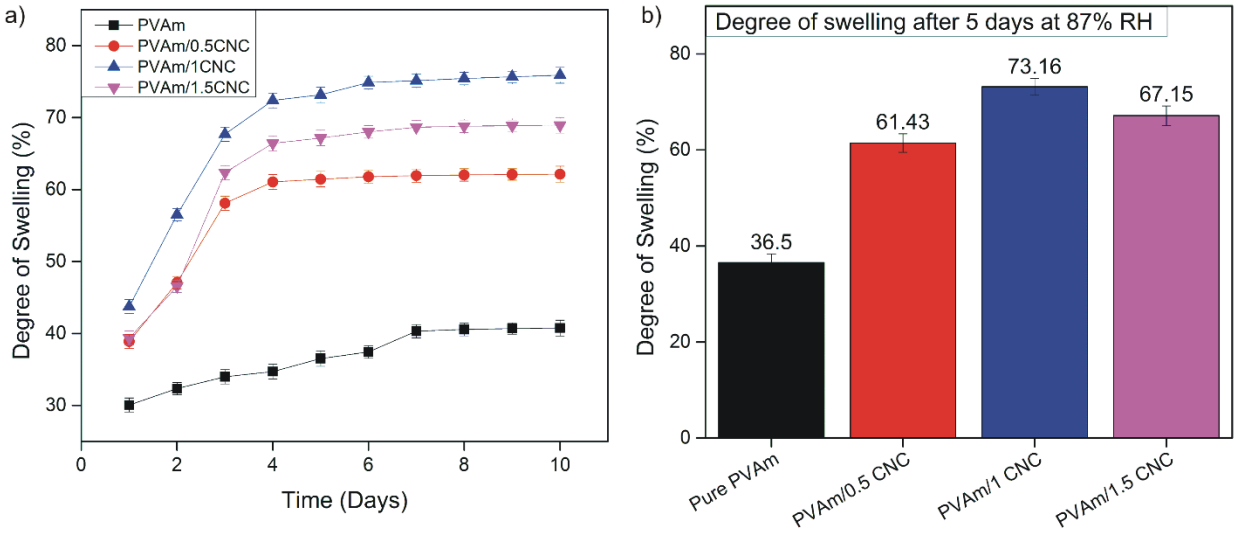

Figure 4. Degree of swelling for ten days (a) degree of swelling of PVAm/CNC membranes compared with pure PVAm membrane at 87% RH (b) maximum degree of swelling after 6 days at 87% RH.

3.1.3 Crystallinity of composite membranes

X-ray diffractogram for pure PVAm and PVAm/CNC composite membranes is shown in figure 5(a). The crystallinity of all composite membranes was calculated as mentioned in section 2.4. At $2\theta = 21.52°$, a sharp peak appeared in all diffractogram which indicated presence of PVAm. The approximate crystallinity of the pure PVAm membrane was calculated around 42%. No peak shift was observed when CNC was added to PVAm membrane. CNC showed its presence on diffractogram in form of a sharp peak at $2\theta = 23.88°$ [38]. This showed that the addition of CNC increased the crystallinity of composite membranes. Figure 5(b) showed the effect of CNC concentration on crystallinity. It was observed that increasing the CNC concentration enhanced the crystallinity of composite membranes. Due to highly crystalline nature of CNC, its peak was visible even at low concentrations [42].

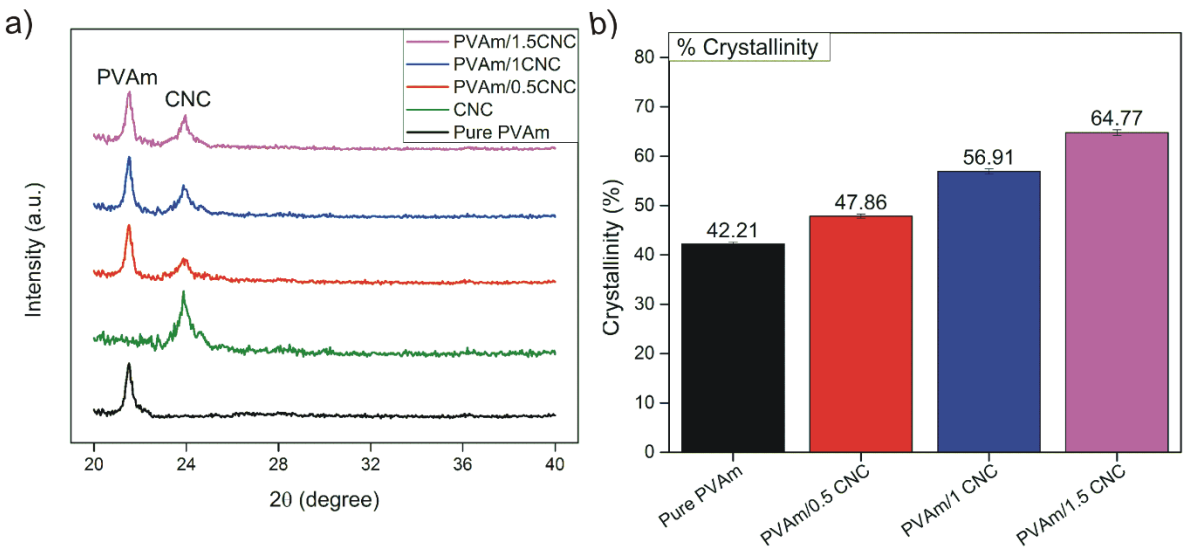

Figure 5. XRD analysis of composite membranes, a) pure PVAm and PVAm/CNC membranes, b) Effect of CNC concentration on % age crystallinity.

PVAm/0.5CNC showed an increased crystallinity as compared to pure PVAm membrane. Maximum crystallinity was attained with addition of 1.5 wt. % CNC in nanocomposite membranes i.e. 64.77 %. Increasing crystallinity imparts rigidity in polymer and inhibits chain mobility.

3.2 Permeation results

3.2.1 CO_2 and CH_4 permeance and selectivity in effect with CNC concentration

Figure 6 shows the effect of increasing CNC concentration on membrane performance in terms of permeance and selectivity for CO_2 and CH_4. Addition of CNC had a positive effect on membrane performance for CO_2 separation. It has been observed that permeance and selectivity of CO_2 enhanced with increasing concentration of CNC in PVAm up to the addition of 1wt% of CNC. From the results as shown in Figure 6 a & c, it has been observed that the pure PVAm membrane showed permeance of 0.00852 m^3(STP)/m^2.bar.hrand selectivity of CO_2/CH_4 around 12at a pressure of 5 bar. Furthermore, the addition of CNC shows enhanced CO_2 permeance and

selectivity for all compositions as compared to pure PVAm. The highest results for CO_2 permeance and CO_2/CH_4 selectivity were obtained by the addition of 1 wt % CNC i.e.0.0216 m^3(STP)/m^2.bar.hr. and41, respectively at 5 bar. However, the decreasing trend has been observed for permeance of CH_4 with increasing CNC concentration. For PVAm/1CNC composite membrane, CH_4 permeance was observed to be 0.000526 m^3(STP)/m^2.bar.hr.at 5 bar.

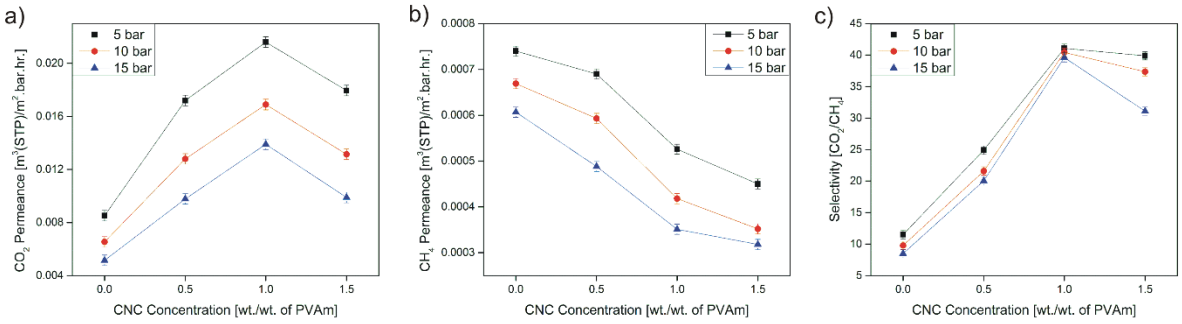

Figure 6. Effect of increasing CNC concentration on permeation performance of PVAm/CNC membranes (a) CO_2 permeance for pure PVAm and PVAm/CNC membranes (b) CH_4 permeance for pure PVAm and PVAm/CNC membranes and (c) Selectivity of $CO_2/CH_4$for pure PVAm and PVAm/CNC membranes.

In addition to membrane structure, the properties of gas pair to be separated is also very important for the performance of membrane. In case of novel composite membranes casted in this work, the separation layer includes polymer phase, dispersed nano filler phase and interaction of these two. In PVAm/CNC composite membranes, the CH_4 is transported only by solution diffusion mechanism. Whereas, in addition to solution diffusion mechanism CO_2 is dominantly transported by facilitated transport mechanism. Addition of CNC in PVAm matrix enhanced the moisture uptake capability of composite membrane. That results in the increased rate of facilitated transport of CO_2. CO_2 is a water soluble gas; therefore, the presence of high water contents increased CO_2 transport in form of bicarbonate ions. Furthermore, the presence of amine groups on backbone of polymeric chain act as fixed carries and selectively transport CO_2 through the membrane. The

chemical equation for the reactions occurring in membrane is defined by the following reactions [10]:

$$-NH_2 + H_2O + CO_2 \rightleftharpoons -NH_3^+ + HCO_3^- \text{ (Upstream side)} \quad (1)$$

$$-NH_3^+ + HCO_3^- \rightleftharpoons -NH_2 + H_2O + CO_2 \text{ (Downstream side)} \quad (2)$$

The addition of CNC in PVAm provides non selective and less resistant pathways for gas transportation. The moisture uptake induces swelling behavior which increases free volume in between the polymeric chains and also increases the chain flexibility. This increases the diffusive transport of gases across the membrane. As the kinetic diameter of CO_2 and CH_4 are 3.3 Å and 3.8 Å, respectively. So, both gases can selectively pass through swelled areas [43]. Even though, the permeance of CO_2 is much higher as compared to CH_4. This can be attributed to the high solubility of CO_2 in water.

Furthermore, it has been observed that the value of permeance for both CO_2 and CH_4 has reduced after addition of CNC above 1 wt%. The decline in membrane performance above 1wt% CNC can be attributed towards the reduced moisture content and increased crystallinity. Increased crystallinity not only induces rigidity in polymer matrix but also reduced moisture uptake ability of composite membranes as explained in section 3.1.3. Therefore, transportation of gas by solution diffusion mechanism has declined. Furthermore, as explained in section 3.3.2 that increasing CNC concentration in PVAm significantly enhanced the selective layer thickness beyond addition of 1wt. % CNC. Hence, it has also contributed to reduce gas permeation through the membrane. The CH_4 permeates only by solution diffusion mechanism due to its non-reactive nature. Hence, its permeance showed sharper decline with increase in chain rigidity. However, the decrease in

moisture uptake ability dominantly affects the transport of CO_2 as it is a water soluble gas and mainly transported through facilitated transport [21].

The transportation mechanism for both the gases is represented in Figure.7. It can be seen that CO_2 is transported by i) reaction with amine carriers present on backbone of polymer matrix. However, due to limited carrier concentration, there will be no further increase in rate of CO_2 transport once a saturation state occurs. This is intrinsic property of PVAm membranes. Addition of CNC had no effect on this property. ii) Transportation of CO_2as bicarbonate ions aids by the presence of moisture contents. Addition of CNC plays significant role in this transport as it enhanced the moisture uptake ability of membrane, and iii) Transport of CO_2 by molecular diffusion. Whereas, the only transport mechanism is molecular diffusion for CH_4.Therefore, addition of 1wt% CNC showed positive effects on CO_2 transport but does not enhance the membrane performance for CH_4 transport.

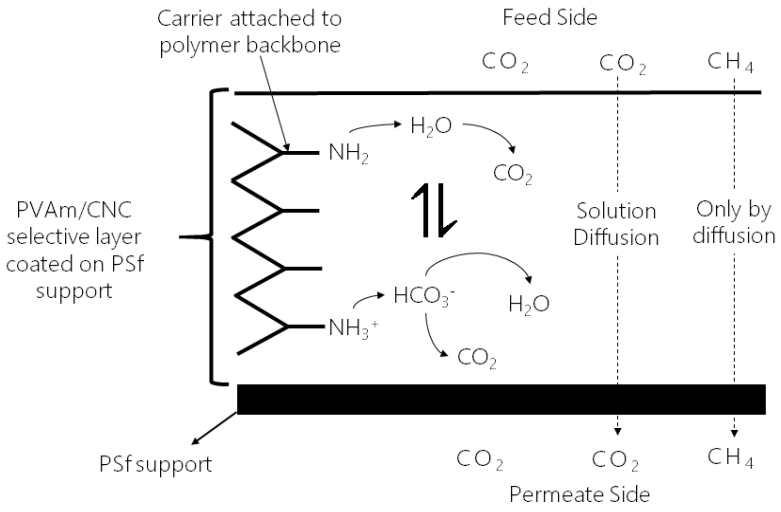

Figure 7. Mechanism of gas transport through PVAm/CNC nanocomposite membranes.

3.2.2 Effect of feed pressure on gas permeance of composite membranes

The pure PVAm and PVAm/CNC composite membranes were tested at a pressure of 5, 10 and 15 bar for CO_2 and CH_4 permeance. It was observed that permeance of both gases and selectivity of CO_2/CH_4 decreased as a result of increasing pressure for all the formulated membranes. The highest CO_2 permeance and CO_2/CH_4selectivity was achieved by PVAm/1CNC membrane at 5 bar pressure i.e. 0.0216 m^3(STP)/m^2.bar.hr. and 41, respectively as shown in Figure 8 (a & c). However, addition of 1wt. % CNC showed decline in permeance ofCH_4using pure PVAm membrane at 5 bar. The values of CH_4 permeance for PVAm and PVAm/1CNC membranes are 0.00074 m^3(STP)/m^2.bar.hr.and 0.000526 m^3(STP)/m^2.bar.hr., respectively. Furthermore, the drop in permeance for CO_2 is rapid in the beginning with increasing pressure. This behavior is attributed to the saturation state of all amine carriers present on polymer matrix. Once the carriers become saturated in pure PVAm membrane, CO_2 is transported only by solution diffusion mechanism. However, the dominating phenomenon is still facilitated transport in PVAm/CNC membranes with aid of moisture content present in membranes. Hence, the values of CO_2 permeance and selectivity of all CNC containing membranes are higher than pure PVAm membranes at all pressure.

Performance of water swollen membranes was high when the feed gas was fully humidified at low pressure. Increased feed pressure enhances the flow of gas. Further high pressure squeezes the membrane and increase the flow of moisture content through the membrane. Hence, moisture contents in the membrane get decreased even at high %RH [17]. Reduction of moisture contents, decrease the facilitated transport of CO_2 across the membrane [12]. Furthermore, at the high feed pressure plasticization occurs in polymeric membranes that reduces the chain mobility and impart

rigidity in membrane structure. This further reduced membrane performance at high pressures [18]. In addition, the high feed pressures introduce compression on polymer matrix that reduces the free voids available for solution diffusion of gases. Hence, results in the decline of permeance of both CO_2 and CH_4. Thus, the decrease in CO_2/ CH_4 selectivity was not very prominent except for PVAm/1.5CNC membrane. The selectivity dropped from 40 to 31 when feed pressure was increased from 5 to 15 bar as shown in Figure 8(c). PVAm/1CNC showed a very minute selectivity drop i.e. 41 to 39, with increase in pressure from 5 to 15 bar.

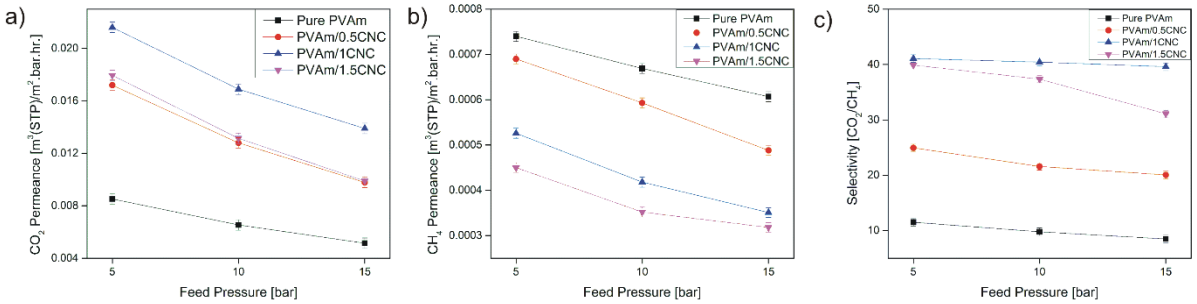

Figure 8. Effect of feed pressure on (a) CO_2 permeance (b) CH_4permeance (c) Selectivity CO_2/CH_4.

3.2.3 Effect of relative humidity on facilitated transport of CO_2

PVAm/1CNC membranes were investigated for the effect of RH on transport of CO_2 and CH_4at 5 bar pressure as shown in figure 9. The effect of %RH was investigated by subjecting the membranes to different humidity levels of 0, 25, 50, 75 and 100% before testing. The different humidity levels were achieved by data obtained from the degree of swelling graphs. Results showed that increasing %RH improved the CO_2 permeance and selectivity. This is due to the fact that higher moisture contents increases facilitated transport of CO_2 across the membrane [40]. Furthermore, an increase in %RH enhances the degree of swelling. Hence, open the amorphous

pores in polymer matrix providing non selective bypass for diffusion ofCO_2 and CH_4 molecules. However, CO_2 moves across the membrane by facilitated and diffusive transport but CH_4 only passes through by diffusive transport. Hence, the increase in CH_4 permeance is very low with a rise in %RH as compare to CO_2 permeance [44]. At 0% RH, CO_2 and CH_4 showed a permeance of 0.00279 m^3(STP)/m^2.bar.hr. and 0.000472 m^3(STP)/m^2.bar.hr., respectively. Increasing the %RH to 100%, CO_2 permeance enhanced approximately 10 folds. While, CH_4 permeance just increased to 0.000526 m^3(STP)/m^2.bar.hr. The rise in the %RH from 0 to 100%, increased the selectivity of membrane from 6 to 41, respectively. High selectivity rise can be attributed to the increase in permeance of CO_2 with rising %RH.

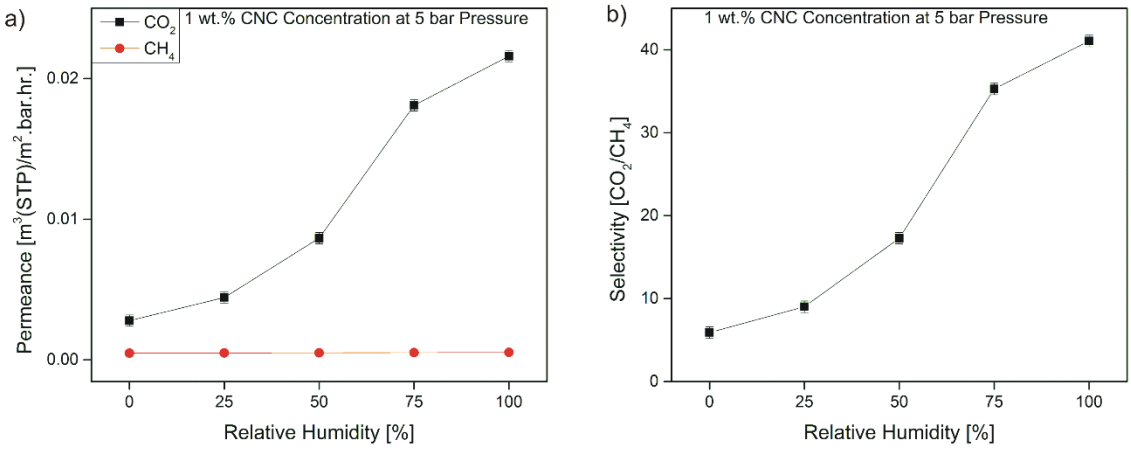

Figure 9. Percentage RH effect on facilitated transport (a) CO_2 and CH_4 permeance (b) CO_2/CH_4 selectivity.

4 Conclusions

PVAm/CNC membranes were successfully fabricated and tested for the effect of CNC concentration and feed pressure on separation performance of CO_2 and CH_4. Addition of CNC has improved the permeance and selectivity of PVAm membrane for CO_2 transport. However, addition of CNC does not showed any significant change on CH_4 permeance. As compared to pure PVAm

membrane, enhanced separation performance was observed when CNC was added in membranes. Furthermore, addition of CNC enhanced the moisture uptake of formulated membranes. The moisture uptake was increased up to the addition of 1 wt.% CNC and started decreasing beyond this concentration. PVAm/1CNC showed a swelling degree of 75.88±1.1%. However, the thickness of selective layer and crystallinity of PVAm/CNC membranes showed increasing trend with increasing CNC concentration. In addition, it was found that by increasing feed pressure the permeance of both gases for the casted membranes declined. However, this decline was more prominent for CH_4 gas. Furthermore, it is highly recommended to work at maximum swollen conditions to get maximum benefit of facilitated transport of CO_2. It was seen that PVAm/1CNC membrane showed the highest CO_2 permeance and selectivity of 0.0216 m^3(STP)/m^2.bar.hr. and 41, respectively at a pressure of 5 bar. According to the results, 1 wt.% CNC was optimized concentration and at 5 bar pressure, membrane showed best results.

References

[1] T.F. Stocker, D. Qin, G.-K. Plattner, M. Tignor, S.K. Allen, J. Boschung, A. Nauels, Y. Xia, V. Bex, P.M. Midgley, Climate change 2013: The physical science basis, Contribution of working group I to the fifth assessment report of the intergovernmental panel on climate change 1535 (2013).

[2] R. Kapoor, P. Ghosh, M. Kumar, V.K. Vijay, Evaluation of biogas upgrading technologies and future perspectives: a review, Environmental Science and Pollution Research 26(12) (2019) 11631-11661.

[3] R. REN21, Global Status Report, REN21 Secretariat, Paris, France, Tech. Rep.2017, pp. 91-93.

[4] B. Kummamuru, WBA global bioenergy statistics 2017, World Bioenergy Association (2016).

[5] E. Santos-Clotas, A. Cabrera-Codony, A. Castillo, M.J. Martín, M. Poch, H. Monclús, Environmental decision support system for biogas upgrading to feasible fuel, Energies 12(8) (2019) 1546.

[6] A.T.A. Felca, R.M. Barros, G.L. Tiago Filho, I.F.S. dos Santos, E.M. Ribeiro, Analysis of biogas produced by the anaerobic digestion of sludge generated at wastewater treatment plants in the South of Minas Gerais, Brazil as a potential energy source, Sustainable cities and society 41 (2018) 139-153.

[7] E. Porpatham, A. Ramesh, B. Nagalingam, Investigation on the effect of concentration of methane in biogas when used as a fuel for a spark ignition engine, fuel 87(8-9) (2008) 1651-1659.

[8] R.W. Baker, K. Lokhandwala, Natural gas processing with membranes: an overview, Industrial & Engineering Chemistry Research 47(7) (2008) 2109-2121.

[9] D. Curto, M. Martín, Renewable based biogas upgrading, Journal of cleaner production 224 (2019) 50-59.

[10] T.J. Kim, B. Li, M.B. Hägg, Novel fixed-site–carrier polyvinylamine membrane for carbon dioxide capture, Journal of Polymer Science Part B: Polymer Physics 42(23) (2004) 4326-4336.

[11] L. Deng, T.-J. Kim, M. Sandru, M.-B. Hägg, PVA/PVAm blend FSC membrane for natural gas sweetening, Proceedings of the 1st annual gas processing symposium, Elsevier, 2009, pp. 247-255.

[12] L. Deng, T.-J. Kim, M.-B.J.J.o.M.S. Hägg, Facilitated transport of CO2 in novel PVAm/PVA blend membrane, 340(1-2) (2009) 154-163.

[13] L. Ansaloni, J. Salas-Gay, S. Ligi, M.G. Baschetti, Nanocellulose-based membranes for CO2 capture, Journal of Membrane Science 522 (2017) 216-225.

[14] D. Romero Nieto, A. Lindbråthen, M.-B.J.A.O. Hagg, Effect of water interactions on polyvinylamine at different pHs for membrane gas separation, 2(11) (2017) 8388-8400.

[15] D. Venturi, D. Grupkovic, L. Sisti, M.G. Baschetti, Effect of humidity and nanocellulose content on Polyvinylamine-nanocellulose hybrid membranes for CO2 capture, Journal of Membrane Science 548 (2018) 263-274.

[16] R. Quinn, J. Appleby, G. Pez, New facilitated transport membranes for the separation of carbon dioxide from hydrogen and methane, Journal of Membrane Science 104(1-2) (1995) 139-146.
[17] X. He, M.J.J.M.S.T. Hägg, Investigation on nanocomposite membranes for high pressure CO2/CH4 separation, 7(169) (2017) 2.
[18] Z. Jahan, M.B.K. Niazi, M.-B. Hägg, Ø.W. Gregersen, Cellulose nanocrystal/PVA nanocomposite membranes for CO2/CH4 separation at high pressure, Journal of membrane science 554 (2018) 275-281.
[19] X. He, A review of material development in the field of carbon capture and the application of membrane-based processes in power plants and energy-intensive industries, Energy, Sustainability and Society 8(1) (2018) 34.
[20] T.-J. Kim, H. Vrålstad, M. Sandru, M.-B. Hägg, Separation performance of PVAm composite membrane for CO2 capture at various pH levels, Journal of membrane science 428 (2013) 218-224.
[21] O.G. Nik, X.Y. Chen, S.J.J.o.M.S. Kaliaguine, Functionalized metal organic framework-polyimide mixed matrix membranes for CO2/CH4 separation, 413 (2012) 48-61.
[22] M. Wang, Z. Wang, N. Li, J. Liao, S. Zhao, J. Wang, S. Wang, Relationship between polymer–filler interfaces in separation layers and gas transport properties of mixed matrix composite membranes, Journal of membrane science 495 (2015) 252-268.
[23] Z. Qiao, Z. Wang, C. Zhang, S. Yuan, Y. Zhu, J. Wang, S. Wang, PVAm–PIP/PS composite membrane with high performance for CO 2/N 2 separation, AIChE Journal 59(1) (2013) 215-228.
[24] D. Venturi, L. Ansaloni, M.G. Baschetti, Nanocellulose based facilitated transport membranes for CO 2 separation, Chemical Engineering Transactions 47 (2016) 349-354.
[25] S. Janakiram, X. Yu, L. Ansaloni, Z. Dai, L. Deng, Manipulation of Fibril Surfaces in Nanocellulose-Based Facilitated Transport Membranes for Enhanced CO2 Capture, ACS applied materials & interfaces 11(36) (2019) 33302-33313.
[26] D. Venturi, A. Chrysanthou, B. Dhuiège, K. Missoum, M. Giacinti Baschetti, Arginine/Nanocellulose Membranes for Carbon Capture Applications, Nanomaterials 9(6) (2019) 877.
[27] B. Dhuiège, E. Lasseuguette, M.-C. Brochier-Salon, M.-C. Ferrari, K. Missoum, Crosslinked Facilitated Transport Membranes Based on Carboxymethylated NFC and Amine-Based Fixed Carriers for Carbon Capture, Utilization, and Storage Applications, Applied Sciences 10(1) (2020) 414.
[28] Z. Jahan, M.B.K. Niazi, Ø.W. Gregersen, Mechanical, thermal and swelling properties of cellulose nanocrystals/PVA nanocomposites membranes, Journal of industrial and engineering chemistry 57 (2018) 113-124.
[29] M.-J. Cho, B.-D. Park, Tensile and thermal properties of nanocellulose-reinforced poly (vinyl alcohol) nanocomposites, Journal of Industrial and Engineering Chemistry 17(1) (2011) 36-40.
[30] Y.C. Ching, T.S. Ng, Effect of preparation conditions on cellulose from oil palm empty fruit bunch fiber, BioResources 9(4) (2014) 6373-6385.

[31] M. Mariano, N. El Kissi, A. Dufresne, Cellulose nanocrystals and related nanocomposites: review of some properties and challenges, Journal of Polymer Science Part B: Polymer Physics 52(12) (2014) 791-806.
[32] S. Kalia, A. Dufresne, B.M. Cherian, B. Kaith, L. Avérous, J. Njuguna, E.J.I.j.o.p.s. Nassiopoulos, Cellulose-based bio-and nanocomposites: a review, 2011 (2011).
[33] L. Han, S. Cui, H.-Y. Yu, M. Song, H. Zhang, N. Grishkewich, C. Huang, D. Kim, K.M.C.J.A.A.M. Tam, Interfaces, Self-healable conductive nanocellulose nanocomposites for biocompatible electronic skin sensor systems, 11(47) (2019) 44642-44651.
[34] M. Song, H. Yu, J. Gu, S. Ye, Y.J.I.j.o.b.m. Zhou, Chemical cross-linked polyvinyl alcohol/cellulose nanocrystal composite films with high structural stability by spraying Fenton reagent as initiator, 113 (2018) 171-178.
[35] D. Rana, B. Mandal, S.J.M. Bhattacharyya, Analogue calorimetric studies of blends of poly (vinyl ester) s and polyacrylates, 29(5) (1996) 1579-1583.
[36] D. Rana, B. Mandal, S.J.P. Bhattacharyya, Analogue calorimetry of polymer blends: poly (styrene-co-acrylonitrile) and poly (phenyl acrylate) or poly (vinyl benzoate), 37(12) (1996) 2439-2443.
[37] D. Rana, B. Mandal, S.J.P. Bhattacharyya, Miscibility and phase diagrams of poly (phenyl acrylate) and poly (styrene-co-acrylonitrile) blends, 34(7) (1993) 1454-1459.
[38] Z. Jahan, M.B.K. Niazi, M.-B. Hägg, Ø.W.J.J.o.m.s. Gregersen, Cellulose nanocrystal/PVA nanocomposite membranes for CO2/CH4 separation at high pressure, 554 (2018) 275-281.
[39] W. Shujun, Y. Jinglin, G.J.A.J.o.B. Wenyuan, Biotechnology, Use of X-ray diffractometry (XRD) for identification of Fritillaria according to geographical origin, 1(4) (2005) 207-211.
[40] Z. Jahan, M.B.K. Niazi, M.-B. Hägg, Ø.W.J.S. Gregersen, P. Technology, Decoupling the effect of membrane thickness and CNC concentration in PVA based nanocomposite membranes for CO2/CH4 separation, 204 (2018) 220-225.
[41] A.J.R.J.o.A.C. Bochek, Effect of hydrogen bonding on cellulose solubility in aqueous and nonaqueous solvents, 76(11) (2003) 1711-1719.
[42] M.R. Kamal, V.J.C.p. Khoshkava, Effect of cellulose nanocrystals (CNC) on rheological and mechanical properties and crystallization behavior of PLA/CNC nanocomposites, 123 (2015) 105-114.
[43] S. Kobayashi, K.-D. Suh, Y. Shirokura, T.J.P.j. Fujioka, Viscosity behavior of poly (vinylamine) and swelling-contraction phenomenon of its gel, 21(12) (1989) 971.
[44] Y. Shen, H. Wang, J. Liu, Y.J.A.S.C. Zhang, Engineering, Enhanced performance of a novel polyvinyl amine/chitosan/graphene oxide mixed matrix membrane for CO2 capture, 3(8) (2015) 1819-1829.